Carrier Frequency Offset Based Robust Radio Frequency Fingerprint for OFDM Communication in Time-Varying Channels

Liu Gengyi[1], Pan Yijin[1], Wang Junbo[1], Chen Yijian[2], Yu Hongkang[2]

(1. National Mobile Communications Research Laboratory, Southeast University, Nanjing 211111, China;
2. Wireless Product Research and Development Institute, ZTE Corporation, Shenzhen 518057, China)

DOI: 10.12142/ZTECOM.202601005

https://kns.cnki.net/kcms/detail/34.1294.TN.20260210.0908.002.html, published online February 10, 2026

Manuscript received: 2025-01-11

Abstract: The radio frequency (RF) fingerprint technique is a robust method for security enhancement of the physical layer by leveraging the unique RF imperfections inherent in various wireless devices. Among these imperfections, the carrier frequency offset (CFO) stands out as a primary RF fingerprint (RFF) of the transmitter, offering the potential to distinguish among different transmitters. However, accurately estimating CFO in time-varying channels poses significant challenges due to multipath effects and Doppler shifts. In this paper, we focus on estimating CFO for wireless device identification in the orthogonal frequency division multiplexing (OFDM) communication system. To achieve precise CFO estimation under time-varying channels, we propose a frequency domain correlation and spline interpolation (FCSI) algorithm. This approach utilizes pilots distributed across different subcarriers to correlate with prior local sequences, facilitating accurate CFO estimation. Classification is then performed based on the Euclidean distance between the prior RFF and the tested RFF dataset. Simulation results demonstrate that the proposed M-consecutive average method effectively reduces the classification error rate in the challenging high-frequency (HF) skywave channel environment.

Keywords: RF fingerprint; RF identification; carrier frequency offset; time-varying channels; OFDM

Citation (Format 1): Liu G Y, Pan Y J, Wang J B, et al. Carrier frequency offset based robust radio frequency fingerprint for OFDM communication in time-varying channels [J]. ZTE Communications, 2026, 24(1): 25 - 33. DOI: 10.12142/ZTECOM.202601005
Citation (Format 2): G. Y. Liu, Y. J. Pan, J. B. Wang, et al., "Carrier frequency offset based robust radio frequency fingerprint for OFDM communication in time-varying channels," *ZTE Communications*, vol. 24, no. 1, pp. 25 - 33, Mar. 2026. doi: 10.12142/ZTECOM.202601005.

1 Introduction

The transmission of wireless communication signals relies on radio frequency (RF) hardware, which is significantly affected by the imperfections of the RF transmitter and receiver. Due to the presence of RF imperfections, the signal received by the receiver inherently carries unique RF fingerprints that can be utilized for transmitter identification. The identification of individual RF transmitters involves extracting and analyzing the unique characteristics of each transmitter through the receiver. This process identifies the different transmitters by analyzing the signals emitted from unknown transmitters. Therefore, the primary focus of RF fingerprint research is to determine which types of RF fingerprints (RFF) are advantageous for the identification of transmitters.

In Ref. [1], RFF extraction methods are categorized into transient-state-based RFF, steady-state-based RFF, and other approaches. Transient-state-based RFF focuses on transition extraction from off to on or the control signal at the transmitter, which occurs before the data transmission of the signal. Ref. [2] extracts the RFF of transmitters from the distance between the start and the end points of the transient signal. Moreover, the normalized amplitude variance, the number of peaks, and the wavelet transform are utilized for the transient RFF. The short-time Fourier transform (STFT) is employed to obtain the spectrum of transient control signals of unmanned aerial vehicles (UAV)[3]. The energy transient is used to extract 15 statistical properties to analyze the control signals of the UAV. Steady-state-based RFF primarily focuses on features extracted from the received modulated signals. Five specific features of RF imperfection are used in a Passive Radiometric Device Identification System (PARADIS) for physical-layer transmitter identification[4]. Differential constellation trace figures (DCTF), carrier frequency offset, modulation offset, and in-phase/quadrature-

This work was supported by ZTE Industry-University-Institute Cooperation Funds under Grant No. IA20240723011, National Natural Science Foundation of China under Grant No. 62371123, Young Elite Scientists Sponsorship Program of the Beijing High Innovation Plan under Grant No. 20251077, and Research Fund of National Mobile Communications Research Laboratory, Southeast University under Grant No. 2023A03.

phase (IQ) offset extracted from constellation trace figures (CTF) serve as steady-state-based RFFs in Ref. [5]. A hybrid classification method is proposed to classify different transmitters by training and testing these steady-state-based RFFs. Moreover, deep learning significantly impacts RF fingerprint techniques. It is particularly effective for classification tasks due to its adaptability to the features in target signals, making it well-suited for RFF applications. In contrast, methods relying on predefined models or features often struggle to accurately detect sufficient distinguishing characteristics among devices[6]. For instance, Ref. [7] examines two CNN models to assess RF fingerprint effectiveness under various environmental conditions, focusing on factors such as channel influence, the signal-to-noise ratio (SNR), the number of devices, and the training dataset size. Ref. [8] introduces a radio frequency fingerprint identification (RFFI) approach for long range (LoRa) systems, leveraging deep learning to enhance security through the identification of devices' unique hardware features. RFFs can also be extracted from channel-based features or channel fingerprints that rely on location features in static scenarios. The radio signal strength indicator (RSSI), which depends on transmit power and channel attenuation, is used as an RFF feature[9]. The channel impulse response (CIR) [10] and channel frequency response (CFR)[11] represent two kinds of channel fingerprints. Another strategy is the active RFF, which involves the deliberate introduction of controllable imperfections at the transmitter[12] or the insertion of unique "signatures" within IQ signals[13]. This method effectively aids in the differentiation and classification of various transmitters.

However, RFF is highly sensitive to time-varying and multipath channels. Considering high frequency (HF) skywave communication, the extraction of steady-state RFF is significantly challenged by the time-varying feature of wireless channels and the severe multipath effects, adversely affecting extraction precision. HF signals can be transmitted over long distances by the reflection of the ionosphere. The ionosphere moves and changes in density, causing Doppler shifts on the reflected HF signals, which complicates the extraction of RFF features. In time-varying channels, the classification accuracy of the RFF directly related to the received IQ signal will greatly degrade. Apart from the impact of time-varying channels, RFF is highly dependent on the structure and RF components of the RF chain. Different RF chain structures entail different signal processing approaches for baseband signals. For example, a superheterodyne transmitter undergoes more spectrum shift operations than a direct conversion transmitter, leading to more complex scenarios of carrier frequency offset.

In this study, we adopt a direct conversion structure for its simplicity. The baseband signal is modeled to include three types of RF imperfections: CFO, IQ imbalance, and direct current (DC) offset. The contributions of this paper are as follows.

1) We extract carrier frequency offset (CFO) as an RFF in an OFDM-modulated, HF skywave time-varying channel communication system. CFO is a robust RFF in time-varying channels.

2) Traditional CFO estimation algorithms, particularly those based on cyclic prefixes and block pilots, generally perform poorly in time-varying channels[14]. Furthermore, these algorithms have phase ambiguity issues during CFO estimation. To address these challenges, we introduce the frequency domain correlation and spline interpolation (FCSI) algorithm, which estimates CFO in the frequency domain by exploiting the correlation between known local sequences and received pilots across different subcarriers. This approach is designed to be robust against time-varying channels.

3) We utilize the Euclidean distance between the prior RFF and the RFF under test for classification purposes. Moreover, the M-consecutive average method is used for feature post-processing. To validate the proposed estimation and classification method, we simulate a scenario involving the identification of 12 individual transmitters in an HF skywave OFDM communication system.

The rest of this paper is organized as follows: Section 2 introduces the signal model with RF imperfections for HF skywave OFDM systems. Section 3 discusses the proposed FCSI algorithm for estimating CFO. Section 4 details the classification algorithm that utilizes CFO as an RFF to distinguish different devices. Simulation results are presented in Section 5, and the paper concludes with remarks in Section 6.

2 Signal Model

In this section, we analyze an HF skywave OFDM communication system impacted by three types of RF imperfections: CFO, IQ imbalance, and DC offset. We first present the direct conversion RF transmitter structure. Then, we introduce the CFO to evaluate its effect on the baseband signal. Following this, IQ imbalance and DC offset are added to the signal model. Finally, the influence of the HF time-varying channel is considered to accurately simulate the received signal which is used to extract RFF.

The adaptive selection of suitable parameters has enabled the effective implementation of OFDM modulation for wideband HF skywave communication[15]. The OFDM modulation is configured with a cyclic prefix (CP) length of N_{CP}, a set number of subcarriers N_{SC}, and a subcarrier spacing of Δf. Pilots are strategically placed at equal intervals among the subcarriers.

2.1 RF Transmitter Structure

The RF transmitter architecture includes all components, ranging from the digital-to-analog converter (DAC) to the transmitting antenna. As depicted in Fig. 1, within the direct conversion RF chain, the digital signal first undergoes conversion to an analog format by the DAC. It then undergoes low-pass filtering and baseband amplification using an amplifier, which serves to eliminate out-of-band noise and boost the signal's strength. Subsequently, the IQ modulator combines two branches of the IQ signals into one stream. An up-converter is

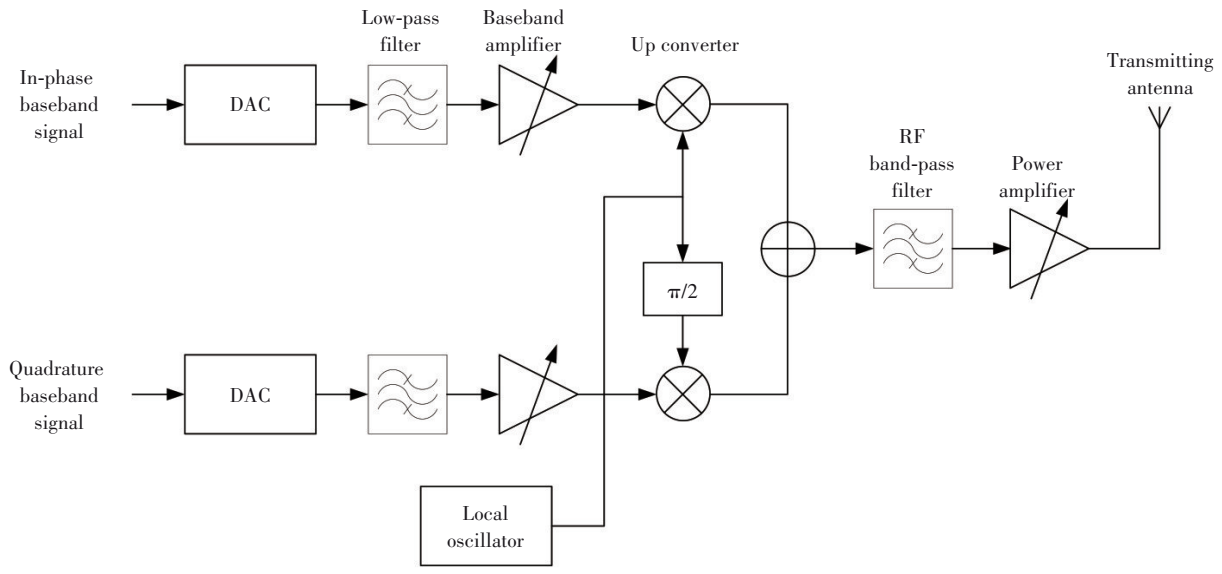

Figure 1. Direct conversion transmitter structure

used for spectrum shift, with the carrier signal produced by a local oscillator. The up-converted signal then passes through an RF band-pass filter and a power amplifier (PA) before being broadcast through the transmitting antenna into the channel.

2.2 Carrier Frequency Offset

CFO typically occurs following the up-conversion process, affected by the characteristics of local oscillators. The natural frequency variation in crystal oscillators causes a persistent difference in the carrier frequencies of the transmitter and receiver. This unique deviation for each transmitter-receiver pair characterizes CFO as a crucial attribute of the transmitter, represented by f_ε. As a result, the up-converted signal x_{CFO}, incorporating the CFO, is expressed as:

$$x_{\mathrm{CFO}} = N\left(x\mathrm{e}^{\mathrm{j}2\pi(f_c+f_\varepsilon)t}\right) \tag{1},$$

where f_c is the carrier frequency and $x = x_r + jx_i$ is the OFDM modulated baseband signal. Considering that the signal transmitted through the channel is a real signal, $N(\cdot)$ signifies taking the real part of a complex number. In the general case, $f_\varepsilon \ll f_c$. Assume that the local oscillator of the down converter in the receiver is perfectly precise, the down-converted signal y is expressed as:

$$y = x_{\mathrm{re}}\mathrm{e}^{-\mathrm{j}2\pi f_c t} \tag{2},$$

where x_{re} is the received signal before the down-conversion. By plugging Eq. (1) into Eq. (2), the down-converted IQ signal y_{IQ} corrupted by carrier frequency offset can be expressed as:

$$y_{\mathrm{IQ}} = \frac{x_r + jx_i}{2}\mathrm{e}^{\mathrm{j}2\pi f_\varepsilon t} + \frac{x_r}{2}\mathrm{e}^{-\mathrm{j}2\pi(2f_c+f_\varepsilon)t} - \frac{jx_i}{2}\mathrm{e}^{-\mathrm{j}2\pi(2f_c+f_\varepsilon)t} \tag{3}.$$

The last two terms of Eq. (3) are filtered out by the low-pass filter. Therefore, Eq. (3) can be modified as:

$$y_{\mathrm{IQ}} = \frac{x_r + jx_i}{2}\mathrm{e}^{\mathrm{j}2\pi f_\varepsilon t} = \frac{x}{2}\mathrm{e}^{\mathrm{j}2\pi f_\varepsilon t} \tag{4}.$$

The spectral shift results in the signal's amplitude being halved and the carrier frequency offset induces a clockwise or counterclockwise rotation, which increases with time in the down-converted IQ signals.

2.3 Other RF Imperfections

Besides CFO, many RF imperfections in the transmitter will corrupt the signal before the signal is transmitted to the channel. Due to the quantization error of DAC and the leakage of the local oscillator, the IQ signals exhibit a notable DC offset denoted by C[16]. Moreover, the gain difference and inexact 90° phase difference may happen to these two signal branches, which will cause IQ imbalance. The IQ parameters are denoted as a_1 and a_2[17]. Therefore, the discrete-time expression of transmitting an IQ signal with DC offset and IQ imbalance can be expressed as follows:

$$X_{\mathrm{IQ}}(n) = \left(a_1 x(n) + a_2 x^*(n)\right) + C \tag{5},$$

where $x(n)$ is the discrete-time expression of the IQ signal from the baseband. Adding the oscillator imperfection CFO, the transmitted signal with RF imperfections after up-conversion

can be modeled as:

$$X_c(n) = N\left(X_{\mathrm{IQ}}(n)e^{\frac{\mathrm{j}2\pi(f_c+f_\varepsilon)n}{F_s}}\right) \tag{6}$$

where $X_c(n)$ is the up-converted signal and F_s is the sample rate.

2.4 HF Skywave Time-Varying Channel

After the up-conversion, the signal goes through the HF skywave channel. In this paper, a wide-sense stationary uncorrelated scattering channel model is considered for the HF skywave channel[18-19]. The intra-path delay can be neglected for the communication signal and the path channel response can be modeled as a time-varying attenuation impulse:

$$c_n(t,\tau) = \alpha_n(t)\delta(\tau) \tag{7}$$

where $\delta(t)$ is the unit-impulse function; τ and $\alpha_n(t)$ are the time delay and impulse of the n-th path, respectively. Assume that the channel is relatively stationary and the relative time delay of each path is independent of time t. The HF skywave channel response can be modeled as:

$$h(t,\tau) = \sum_n c_n(t,\tau-\tau_n) = \sum_n \alpha_n(t)\delta(\tau-\tau_n) \tag{8}$$

We perform the Fourier transform to get the time-varying frequency response:

$$H(f,t) = \int_{-\infty}^{\infty}\sum_n \alpha_n(t)\delta(\tau-\tau_n)\mathrm{e}^{-\mathrm{j}2\pi\tau f}\mathrm{d}\tau = \sum_n \alpha_n(t)\mathrm{e}^{-\mathrm{j}2\pi\tau f} \tag{9}$$

In Eq. (9), the amplitude and phase of the signal are modulated by $\alpha_n(t)$, which is a complex Gaussian random process. The spectrum of $\alpha_n(t)$ follows a Gaussian Doppler spectrum, which can be expressed as:

$$S_G(f) = \frac{1}{\sqrt{2\pi\sigma_G^2}}\mathrm{e}^{-\frac{(f-f_0)^2}{2\sigma_G^2}} \tag{10}$$

where f_0 is the center frequency of the Doppler frequency shift and σ_G is the normalized standard deviation, which is relative to the Doppler spectrum spread f_d.

We can simplify Eq. (8) as:

$$h(t) = \sum_n h_n(t)\delta(t-\tau_n)\mathrm{e}^{\mathrm{j}2\pi f_{dn}t} \tag{11}$$

where $h_n(t)$ and f_{dn} are the n-th path amplitude channel gain and Doppler frequency shift, respectively; f_{dn} is time-varying and Gaussian distributed with f_0 mean and σ_G^2 variance. The discrete-time expression of Eq. (11) is given by:

$$h(n) = \sum_{i=1}^{M_h} h_i(n)\delta(n-D_i)\mathrm{e}^{\frac{\mathrm{j}2\pi f_{di}n}{F_s}} \tag{12}$$

where D_i is the discrete-time form of the time delay and M_h is the number of paths; f_{di} is the Doppler frequency shift corresponding to the i-th path.

Therefore, the received signal $Y(n)$ through the HF skywave channel and additive white Gaussian noise (AWGN) $\omega(n)$ is given by:

$$Y(n) = h(n)*X_c(n) + \omega(n) \tag{13}$$

where * denotes convolution and $\omega(n)\sim N(0,\sigma_N^2)$. Therefore, we can extract RFF from the steady-state received OFDM signal.

3 RFF Extraction Algorithm Design

To precisely estimate the CFO as an RFF in the HF skywave time-varying channel, we propose the FCSI algorithm. The algorithm operates in two stages: first, a frequency domain correlation method is employed to achieve coarse CFO estimation; subsequently, cubic spline interpolation is utilized to refine the estimation for fine CFO correction.

3.1 Frequency Domain Correlation

In OFDM systems, the pilots and the cyclic prefix can be used for the estimation of frequency offsets. In the FCSI algorithm, pilots are employed to correlate with the prior local sequence, thereby extracting the actual frequency offset component. It is assumed that timing synchronization in the OFDM system is perfect. By plugging Eq. (6) and Eq. (13) into Eq. (2), the resultant IQ signal, subjected to a low-pass filtering process, can be written as:

$$Y_{\mathrm{IQ}}(n) = h(n)*\frac{X_{\mathrm{IQ}}(n)}{2}\mathrm{e}^{\frac{\mathrm{j}2\pi f_\varepsilon n}{F_s}} + \omega(n) \tag{14}$$

Without considering the influence of noise, the prior local synchronization sequence, denoted as $x_H(n) = x(n)$, $n = 0,\cdots,L-1$, undergoes a correlation process with the received IQ signal, as specified in Eq. (14). Consequently, the correlation process can be represented as:

$$z(k) = \sum_{n=0}^{L-1} Y_{\mathrm{IQ}}(n+k)x_H^*(n) \tag{15}$$

We assume that the prior local synchronization sequence is the first L symbols of the transmitted IQ signal on the corresponding subcarrier. When $k = 0$, the synchronization is perfect and Eq. (15) can be expanded as follows:

$$z(0) = \sum_{n=0}^{L-1} \frac{h(n)}{2}*X_{\mathrm{IQ}}(n)x^*(n)\mathrm{e}^{\frac{\mathrm{j}2\pi f_\varepsilon n}{F_s}} \tag{16}$$

In the direct conversion communication system, to maintain

communication performance, the IQ amplitude imbalance should be kept below 5 dB, while the phase imbalance should be limited to less than 5°[16], which means that $a_1 \gg a_2$. Moreover, DC offset is calibrated at the receiver and its impact on system performance is smaller than that of IQ imbalance, so that $a_1 \gg C$. Therefore, $X_{\mathrm{IQ}}(n)x^*(n)$ can be expanded as:

$$X_{IQ}(n)x^*(n) = a_1 x(n)x^*(n) + a_2\left[x^*(n)\right]^2 + Cx^*(n) \approx a_1 x(n)x^*(n) = a_1\left|x(n)\right|^2 \quad (17).$$

By plugging Eq. (17) into Eq. (16), $z(0)$ is rewritten as:

$$z(0) = \sum_{n=0}^{L-1}\frac{h(n)}{2} * a_1\left|x(n)\right|^2 \mathrm{e}^{\mathrm{j}2\pi f_\varepsilon \frac{n}{F_s}} \quad (18).$$

In this form, the frequency offset is mainly influenced by the Doppler frequency shift f_{dn} of the HF skywave channel $h(n)$ and the frequency deviation f_ε between the transmitter and receiver. Then we perform N-point fast Fourier transform (FFT) to get the frequency spectrum $Z(f_n)$ of Eq. (18).

$$f_n = \left(n - \frac{N}{2}\right)R_f,\ n = 1,\cdots,N \quad (19),$$

where $R_f = R/N$ is the frequency resolution depending on the symbol rate R and the point number of FFT N. The carrier frequency offset is estimated in the frequency domain, which can be expressed as:

$$F_{\mathrm{coarse}} = \arg\max_{f_n} Z(f_n) \quad (20).$$

Therefore, the coarse estimated frequency offset F_{coarse} of the transmitted signal can be compensated as:

$$Y_{\mathrm{FOcomp}}(n) = Y_{\mathrm{IQ}}(n)\mathrm{e}^{-\mathrm{j}2\pi F_{\mathrm{coarse}}\frac{n}{F_s}} \quad (21).$$

Then we use Eq. (21) to estimate the fine carrier frequency offset.

3.2 Cubic Spline Interpolation

After coarse frequency offset estimation, cubic spline interpolation is used for fine estimation. First, a frequency offset detection range and its step are determined by R_f in Eq. (19). The range is set as $\left[-R_f/2, R_f/2\right]$ and the step is set as R_f/N_R, where N_R is the detection number. Therefore, the detection range can be expressed as:

$$F_{\mathrm{det}}(i) = -\frac{R_f}{2} + (i-1)\frac{R_f}{N_R - 1},\ i = 1,\cdots,N_R \quad (22).$$

Then, we use Eq. (22) to compensate for the frequency offset of the synchronized received IQ sequence in Eq. (21), which can generate N_R IQ signals with different compensated frequency offsets. The inner product of the compensated IQ sequence and the local synchronization sequence is calculated as the correlation peak sequence corresponding to the fine frequency offset detection range. The correlation peak sequence is given by:

$$V_{\mathrm{Peak}}(i) = \sum_{n=0}^{L-1} Y_{\mathrm{FOcomp}}(n)\mathrm{e}^{-\mathrm{j}2\pi F_{\mathrm{det}}(i)\frac{n}{F_s}} x_H^*(n) \quad (23),$$

where $i = 1,\cdots,N_R$. Next, we use the cubic spline interpolation algorithm[20] to fit a finer correlation peak sequence. The detection range $\left[-R_f/2, R_f/2\right]$ is evenly divided into N_S parts and the second derivatives at the boundary $-R_f/2$ and $R_f/2$ are both set to 0. The correlation peak sequence can be interpolated as shown in Fig. 2. We can obtain the finely estimated CFO F_{fine} from the maximum value of the interpolated correlation peak sequence:

$$F_{\mathrm{fine}} = \arg\max_{F_{\mathrm{det}}(i)} V_{\mathrm{Peak}}(i) \quad (24).$$

3.3 FCSI Algorithm

Following the coarse estimation of CFO using frequency domain correlation and subsequent fine CFO estimation through cubic spline interpolation, the accurately estimated CFO F_{est} is obtained by:

$$F_{\mathrm{est}} = F_{\mathrm{coarse}} + F_{\mathrm{fine}} \quad (25),$$

which is the RFF of the transmitter. The flowchart for the FCSI algorithm is depicted in Fig. 3.

As discussed in Section 2, CFO is associated with both the Doppler frequency shift and the frequency deviations in oscillators between the transmitter and the receiver. In HF communication systems, the frequency shift caused by Doppler effects in

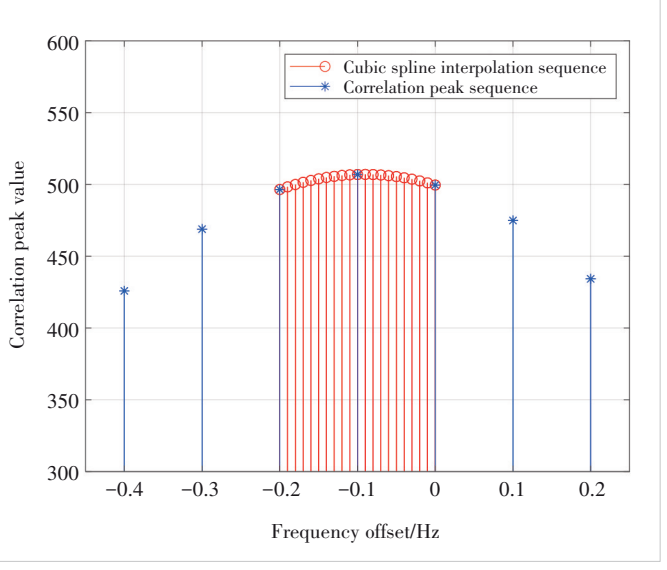

Figure 2. Correlation peak sequence interpolation

time-varying channels is considerably smaller than oscillator frequency deviations. Consequently, frequency domain correlation can accurately determine the primary frequency offset resulting from these deviations. Cubic spline interpolation can estimate fine frequency offsets, thereby making the FCSI algorithm an accurate approach for CFO estimation. Moreover, the CFO is estimated and compensated during the time and frequency synchronization of the received signal, ensuring that this RFF extraction design will not introduce additional computational load. As a result, CFO serves as an effective RFF for distinguishing between different transmitters in HF skywave OFDM communication systems. The complete FCSI algorithm for CFO estimation is summarized as follows.

Algorithm 1. FCSI algorithm for CFO estimation

Input: $Y_{\mathrm{IQ}}(n)$ and $x_H(n)$.

Use Eq. (15) to correlate $Y_{\mathrm{IQ}}(n)$ and $x_H(n)$.

FFT is applied to find the coarse frequency offset by Eq. (18).

Obtain the coarse CFO by Eq. (20).

Obtain the correlation peak sequence in Eq. (23) corresponding to Eq. (22).

Use cubic spline interpolation to estimate fine CFO in Eq. (24) and total estimated CFO in Eq. (25).

Output: Total estimated frequency offset F_{est}.

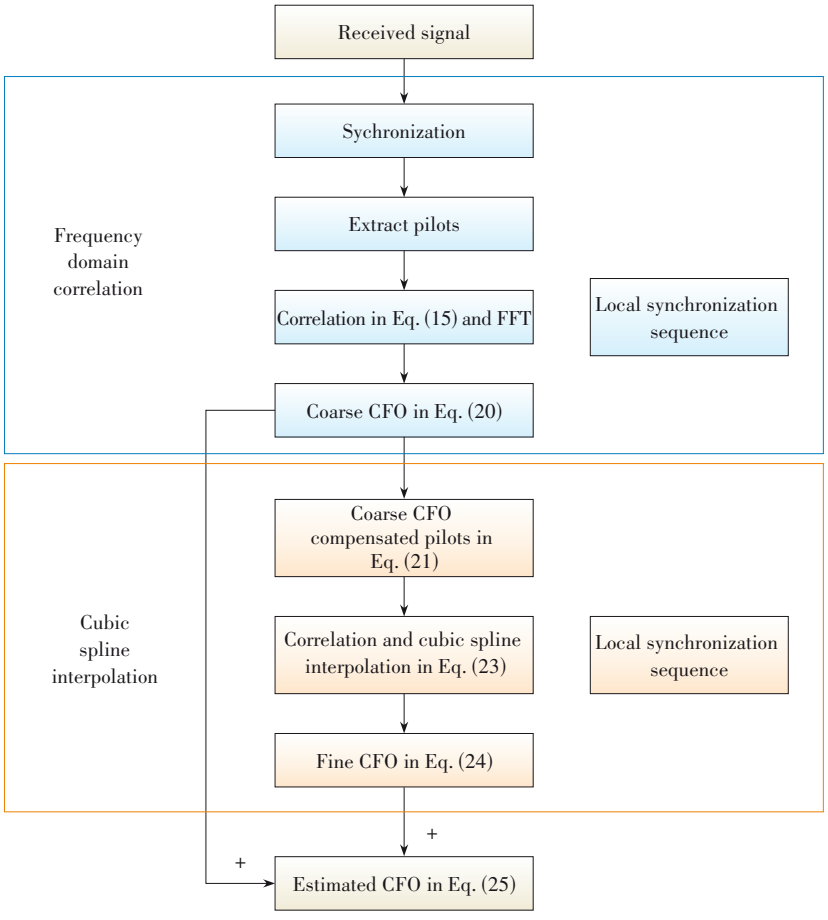

CFO: carrier frequency offset FFT: fast Fourier transform

Figure 3. Frequency domain correlation and spline interpolation algorithm flowchart

4 Classification Algorithm

In this paper, the classification algorithm employs the Euclidean distance to classify RFF and identify the transmitter of a steady-state received signal. The precise relative deviation ΔR_i, $i = 1,\cdots, N_T$ of the oscillators between the transmitter and the receiver used in the classification test can be measured through the direct connection, where N_T is the number of transmitters. Therefore, the prior RFF of each transmitter can be denoted as $\Phi_i = f_c \Delta R_i$, $i = 1,\cdots, N_T$, which is the precise CFO of the 12 transmitters Tx_i, $i = 1,\cdots, N_T$.

Next, we can use the same receiver to receive the signal from different unidentified devices Tx_j, $j \in 1,\cdots, N_T$, from which the CFO $\Phi_{\mathrm{test},j}$ is extracted and identified through the Euclidean distance d_{ji} between the extracted CFO and the prior RFFs Φ_i, which is given by:

$$d_{ji} = |\Phi_{\mathrm{test},j} - \Phi_i|,\ i = 1,\cdots, N_T \quad (26),$$

where the transmitter number corresponding to the prior RFF with the minimal Euclidean distance is denoted as the judgment result k:

$$k = \arg\min_i d_{ji},\ i = 1,\cdots, N_T \quad (27).$$

A classification error is noted when $k \neq j$, indicating an error associated with the received signal from Tx_j. This framework facilitates the classification of signals from each transmitter via the estimated CFO. The number of classification errors and the total test signals from Tx_j are represented by N_{error} and N_{test}, respectively. Therefore, the classification error rate (CER) can be expressed as:

$$\mathrm{CER} = \frac{N_{\mathrm{error}}}{N_{\mathrm{test}}} \quad (28).$$

In this scheme, a CFO extracted from an OFDM modulated frame constitutes one classification sample. Alternatively, the mean of M CFOs extracted from M consecutive frames in the time domain can be considered as a classification sample, where M denotes the sample period. This M-consecutive average method reduces the influence of estimation deviations on classification. The averaged RFFs are represented as

$\bar{\Phi}_{j,l}$, $j \in 1,\cdots,N_T$, $l = 1,2,\cdots,N_F/M$ and $N_{\text{test}} = N_F N_T/M$, where N_F signifies the total number of transmitted frames. By utilizing averaging to reduce the error in frequency offset estimation, this method enables more accurate classification of different transmitters, proving particularly effective in HF skywave channels affected by Doppler spread.

5 Simulation Results

The classification test is conducted with $N_T = 12$ devices, and the simulation parameters are detailed in Table 1. Typically, the frequency tolerance of crystal oscillators varies between −2 and 2 parts per million (ppm). As a result, the corresponding CFO spans from −32 Hz to 32 Hz. Moreover, the ionospheric Doppler shift varies from −1 Hz to 1 Hz in general in the HF skywave channel. The proposed FCSI CFO estimation method is labeled as FCSI. For comparison, the performance of both block pilot (BP)-based and CP-based CFO estimation is simulated, which are labeled as BP and CP, respectively.

A single CFO is estimated from one frame with a synchronization header in the different subcarriers. We conduct CFO estimations using 8 pilots in corresponding subcarriers from 1 000 frames for each transmitter. Following this, we estimate the CFO for $N_F = 1\,000$ frames per transmitter to conduct the classification test. Eqs. (26) and (27) are employed to calculate the number of classification errors, with $N_{\text{test}} = N_F N_T/M$.

Figs. 4 and 5 indicate that the CER is closely related to the mean squared error (MSE) of the CFO estimation algorithm in both HF and AWGN channels. Notably, the CER achieved by the FCSI-based estimation is substantially lower than that obtained using CP-based and BP-based methods, highlighting the superior performance of the FCSI algorithm. Fig. 5 presents the simulated CER in an AWGN channel. The FCSI algorithm demonstrates superior CER performance compared with both BP-based and CP-based algorithms. In the AWGN channel, the absence of Doppler spread means that the estimated frequency offset is free from frequency errors attributable to the channel. The absence of Doppler spread results in an overall CER that is lower than that observed in HF channel, as illustrated in Fig. 4. The CFO estimation in the HF skywave channel is affected by the Gaussian distribution of Doppler shifts, leading to the convergence of the MSE of the FCSI algorithm as the SNR increases, which in turn prevents the CER from decreasing with higher SNR. The MSE of CFO at an SNR of 16 dB is 0.204 7, which is very close to the set Gaussian distributed Doppler shift variance $\sigma_G^2 = 0.25$. This result demonstrates the effectiveness of the FCSI method for CFO estimation. In such scenarios, the actual CFO difference between devices is smaller than the Doppler shift induced by the HF skywave channel, complicating the classification of devices with similar CFOs. Therefore, we need to mitigate the impact of Doppler spread. Considering the distribution of the Doppler

Table 1. Simulation system parameters of the classification test

Parameter	Value
Device number N_T	12
HF channel multipath number	2
Multipath delay τ	2 ms
Standard deviation of Doppler shift σ_G	0.5
Carrier frequency f_c	16 MHz
System bandwidth BW	320 kHz
Subcarrier spacing Δf	500 Hz
Subcarrier number N_{SC}	512
CP length N_{CP}	8
Guard band subcarrier number	50

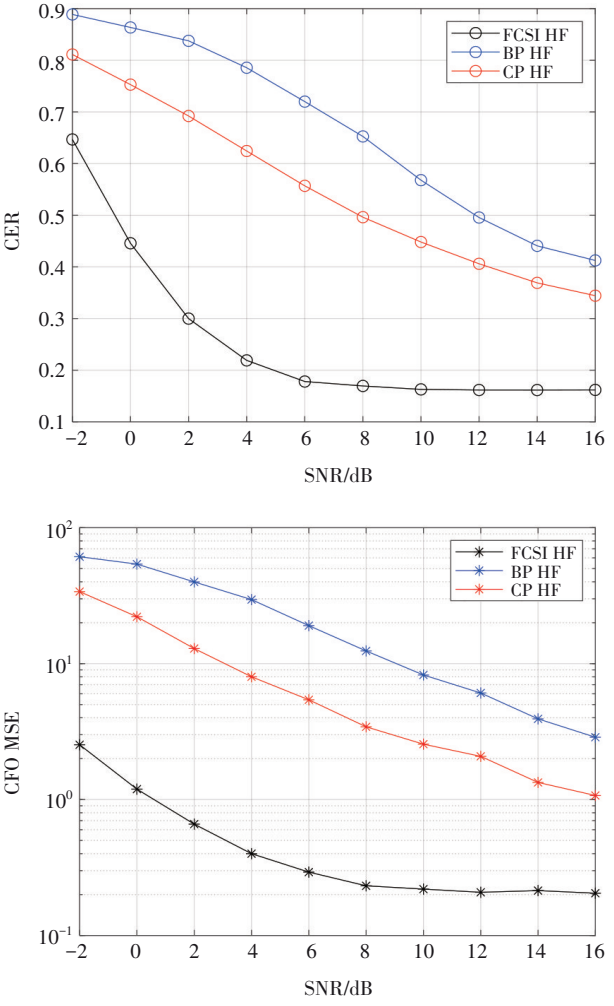

BP: block pilot
CER: classification error rate
CFO: carrier frequency offset
CP: cyclic prefix
FCSI: frequency domain correlation and spline interpolation
HF: high frequency
MSE: mean squared error
SNR: signal-to-noise ratio

Figure 4. CER and MSE of CFO estimation with different SNRs in HF channel

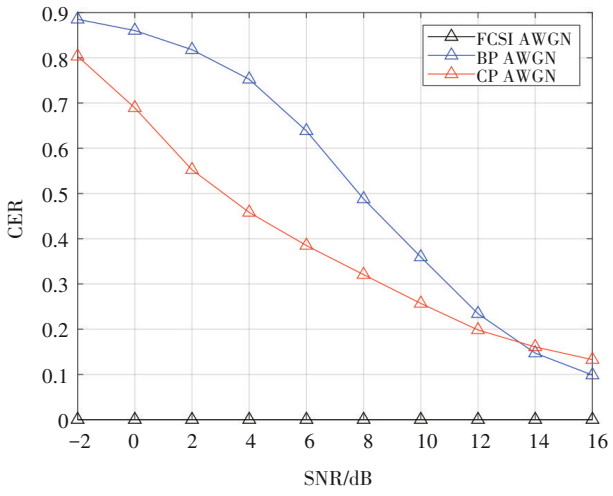

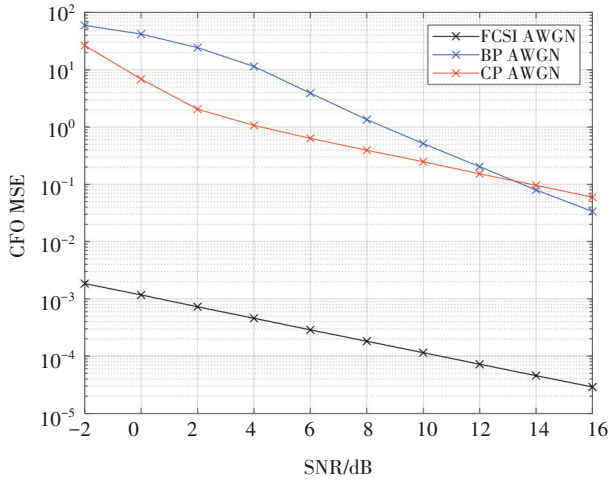

AWGN: additive white Gaussian noise
BP: block pilot
CER: classification error rate
CFO: carrier frequency offset
CP: cyclic prefix
FCSI: frequency domain correlation and spline interpolation
MSE: mean squared error
SNR: signal-to-noise ratio

Figure 5. CER and MSE of CFO estimation with different SNRs in AWGN channel

shift, we can use the M-consecutive average method to leverage statistical properties and appropriately reduce the randomness of the Doppler shift.

The M-consecutive average method is applied to the classification in the HF skywave channel. As shown in Figs. 8 and 9, the CER and MSE of the CFO estimation decrease with the increasing M, demonstrating the effectiveness of this method in reducing the CER of classification in the channel. When M = 16, the CER of the FCSI algorithm can reach 9.47% at an SNR of 10 dB. The experimental results indicate that leveraging the statistical properties of CFO effectively mitigates the impact of the Doppler shift on device identification, significantly reducing the CER.

6 Conclusions

We introduce DC offset, IQ imbalance, and CFO into the baseband signal to simulate the impact of RF imperfections on an HF skywave time-varying channel in the OFDM system. We employ an HF skywave channel model characterized by random Doppler frequency shifts and propose the FCSI algorithm to estimate the CFO of the transmitter as the RFF. Subsequently, the Euclidean distance between prior and test RFFs is used to classify 12 transmitters. The simulation results demonstrate that the FCSI method achieves a significantly lower CER than those obtained by CP- and BP-based CFO estimation methods. Furthermore, the M-consecutive average method proves to be an effec-

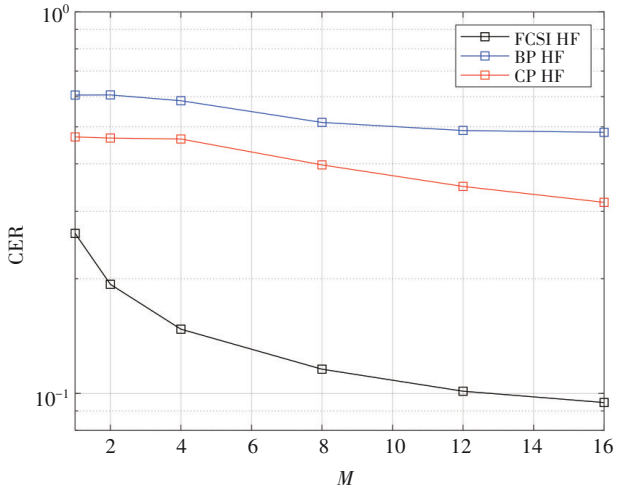

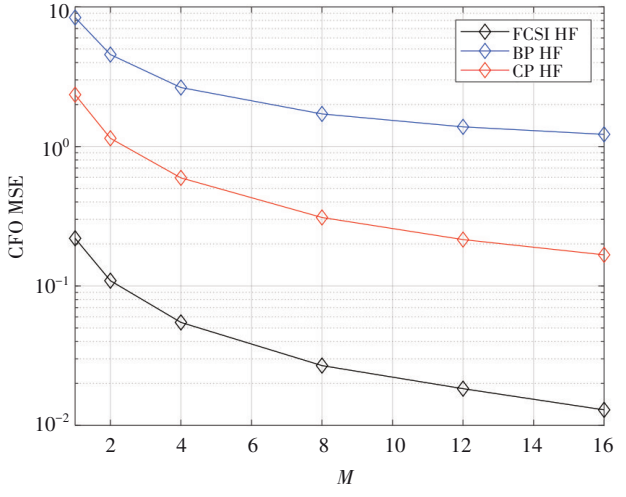

BP: block pilot
CER: classification error rate
CFO: carrier frequency offset
CP: cyclic prefix
FCSI: frequency domain correlation and spline interpolation
HF: high frequency
MSE: mean squared error

Figure 8. CER and MSE of CFO estimation versus M in HF channel

tive strategy for reducing the CER in the HF skywave channel to resist the influence of Doppler spread on RFF extraction.

References

[1] Soltanieh N, Norouzi Y, Yang Y, et al. A review of radio frequency fingerprinting techniques [J]. IEEE journal of radio frequency identification, 2020, 4(3): 222 – 233. DOI: 10.1109/JRFID.2020.2968369
[2] Bonne R K, Capkun S. Implications of radio fingerprinting on the security of sensor networks [C]//The Third International Conference on Security and Privacy in Communications Networks and the Workshops. IEEE, 2007: 331 – 340. DOI: 10.1109/SECCOM.2007.4550352
[3] Ezuma M, Erden F, Kumar A C, et al. Detection and classification of UAVs using RF fingerprints in the presence of Wi-Fi and bluetooth interference [J]. IEEE open journal of the communications society, 2020, 1: 60 – 76. DOI: 10.1109/OJCOMS.2019.2955889
[4] Brik V, Banerjee S, Gruteser M, et al. Wireless device identification with radiometric signatures [C]//The 14th ACM International Conference on Mobile Computing and Networking. ACM, 2008: 116 – 127. DOI: 10.1145/1409944.1409959
[5] Peng L N, Hu A Q, Zhang J Q, et al. Design of a hybrid RF fingerprint extraction and device classification scheme [J]. IEEE Internet of Things journal, 2019, 6(1): 349 – 360. DOI: 10.1109/JIOT.2018.2838071
[6] Merchant K, Revay S, Stantchev G, et al. Deep learning for RF device fingerprinting in cognitive communication networks [J]. IEEE journal of selected topics in signal processing, 2018, 12(1): 160 – 167. DOI: 10.1109/JSTSP.2018.2796446
[7] Jian T, Rendon B C, Ojuba E, et al. Deep learning for RF fingerprinting: a massive experimental study [J]. IEEE Internet of Things magazine, 2020, 3(1): 50 – 57. DOI: 10.1109/IOTM.0001.1900065
[8] Shen G X, Zhang J Q, Marshall A, et al. Radio frequency fingerprint identification for LoRa using deep learning [J]. IEEE journal on selected areas in communications, 2021, 39(8): 2604 – 2616. DOI: 10.1109/JSAC.2021.3087250
[9] Yiu S, Dashti M, Claussen H, et al. Wireless RSSI fingerprinting localization [J]. Signal processing, 2017, 131: 235 – 244. DOI: 10.1016/j.sigpro.2016.07.005
[10] Liu F J, Wang X B, Primak S L. A two dimensional quantization algorithm for CIR-based physical layer authentication [C]//International Conference on Communications (ICC). IEEE, 2013: 4724 – 4728. DOI: 10.1109/ICC.2013.6655319
[11] Xiao L, Li Y, Han G A, et al. PHY-layer spoofing detection with reinforcement learning in wireless networks [J]. IEEE transactions on vehicular technology, 2016, 65(12): 10037 – 10047. DOI: 10.1109/TVT.2016.2524258
[12] Sankhe K, Belgiovine M, Zhou F, et al. ORACLE: optimized radio classification through convolutional neural networks [C]//IEEE Conference on Computer Communications. IEEE, 2019: 370 – 378. DOI: 10.1109/infocom.2019.8737463
[13] Mohanti S, Soltani N, Sankhe K, et al. AirID: injecting a custom RFF for enhanced UAV identification using deep learning [C]//Global Communications Conference. IEEE, 2020: 1 – 6. DOI: 10.1109/GLOBECOM42002.2020.9322561
[14] Van de Beek J J, Sandell M, Borjesson P O. ML estimation of time and frequency offset in OFDM systems [J]. IEEE transactions on signal processing, 1997, 45(7): 1800 – 1805. DOI: 10.1109/78.599949
[15] Yu X L, Lu A N, Gao X Q, et al. HF skywave massive MIMO communication [J]. IEEE transactions on wireless communications, 2022, 21(4): 2769 – 2785. DOI: 10.1109/TWC.2021.3115820
[16] Gu Q Z. RF system design of transceivers for wireless communications [M]. New York: Springer-Verlag, 2005. DOI: 10.1007/b104642
[17] Zhang W C, de Lamare R C, Pan C H, et al. Widely linear precoding for large-scale MIMO with IQI: algorithms and performance analysis [J]. IEEE transactions on wireless communications, 2017, 16(5): 3298 – 3312. DOI: 10.1109/TWC.2017.2679706
[18] Watterson C, Juroshek J, Bensema W. Experimental confirmation of an HF channel model [J]. IEEE transactions on communication technology, 1970, 18(6): 792 – 803. DOI: 10.1109/TCOM.1970.1090438
[19] Mastrangelo J F, Lemmon J J, Vogler L E, et al. A new wideband high frequency channel simulation system [J]. IEEE transactions on communications, 1997, 45(1): 26 – 34. DOI: 10.1109/26.554283
[20] Mckinley S, Levine M. Cubic spline interpolation [M]. [S.l.]: College of the Redwoods, 1998
[21] Zeng C, Wang J B, Xiao M, et al. Task-oriented semantic communication over rate splitting enabled wireless control systems for URLLC services [J]. IEEE transactions on communications, 2024, 72(2): 722 – 739. DOI: 10.1109/TCOMM.2023.3325901
[22] Gong P Y, Zhang G D, Zhang G. Research on fall detection system based on commercial Wi-Fi devices [J]. ZTE communications, 2023, 21(4): 60 – 68. DOI: 10.12142/ZTECOM.202304008
[23] Wu J Y, Wang C Y, Xie L. Device-free in-air gesture recognition based on RFID tag array [J]. ZTE communications, 2021, 19(3): 13 – 21. DOI: 10.12142/ZTECOM.202103003
[24] Zhu Y T, Li Z, Zhang H T. Robust beamforming under channel prediction errors for time-varying MIMO system [J]. ZTE communications, 2023, 21(3): 77 – 85. DOI: 10.12142/ZTECOM.202303011

Biographies

Liu Gengyi received his BS degree from the School of Information Science and Engineering, Southeast University, China in 2022, where he is pursuing his ME degree. His research interests include reconfigurable intelligent surfaces (RIS), mmWave communications, and radio frequency fingerprint (RFF) identification.

Pan Yijin received her BS and MS degrees in communication engineering from Chongqing University, China in 2011 and 2014, respectively, and PhD degree from the School of Information Science and Engineering, Southeast University, China in 2018, where she is currently an associate professor. She was a recipient of Royal Society Newton International Fellowship (2019 – 2021), UK. Her research focuses on key technologies for future communication networks, specifically for edge intelligence-enhanced communication schemes. She serves as a reviewer and a TPC member for prestigious international journals and conferences.

Wang Junbo (jbwang@seu.edu.cn) received his BS degree in computer science from Hefei University of Technology, China in 2003 and PhD degree in communications engineering from Southeast University, China in 2008. From October 2008 to August 2013, he was with Nanjing University of Aeronautics and Astronautics, China. From February 2011 to February 2013, he was a post-doctoral fellow with the National Laboratory for Information Science and Technology, Tsinghua University, China. Since August 2013, he has been an associate professor with the National Mobile Communications Research Laboratory, Southeast University. From October 2016 to September 2018, he was awarded the Marie Skłodowska-Curie Actions Fellowships and a worked as a research fellow with the University of Kent, UK. His current research interests include cloud radio access networks, mmWave communications, and wireless optical communications.

Chen Yijian graduated from Central South University, China. He is currently working at ZTE Corporation. His research interests include reconfigurable intelligent metasurfaces, extremely large-scale MIMO technology, and electromagnetic information theory.

Yu Hongkang received his BS degree from Beijing Jiaotong University, China in 2016 and PhD degree from Peking University, China in 2021. He is currently an engineer with ZTE Corporation. His current research interests include mmWave, massive MIMO, and channel estimation.